

# FRET Nanoflares for Intracellular mRNA Detection: Avoiding False Positive Signals and Minimizing Effects of System Fluctuations

Yanjing Yang,<sup>‡</sup> Jin Huang,<sup>‡</sup> Xiaohai Yang, Ke Quan, He Wang, Le Ying, Nuli Xie, Min Ou, and Kemin Wang\*

State Key Laboratory of Chemo/Biosensing and Chemometrics, College of Chemistry and Chemical Engineering, Key Laboratory for Bio-Nanotechnology and Molecular Engineering of Hunan Province, Hunan University, Changsha 410082, P. R. China

**S** Supporting Information

**ABSTRACT:** A new class of intracellular nanoprobe, termed fluorescence resonance energy transfer (FRET) nanoflares, was developed to sense mRNA in living cells. It consists of a gold nanoparticle (AuNP), recognition sequences, and flares. Briefly, the AuNP functionalized with recognition sequences hybridized to flares, which are designed as hairpin structures and fluorescently labeled donors and acceptors at two ends, respectively. In the absence of targets, the flares are captured by binding with the recognition sequences, separating of the donor and acceptor, and inducing low FRET efficiency. However, in the presence of targets, the flares are gradually displaced from the recognition sequences by the targets, subsequently forming hairpin structures that bring the donor and acceptor into close proximity and result in high FRET efficiency. Compared to the conventional single-dye nanoflares, the upgraded FRET nanoflares can avoid false positive signals by chemical interferences (such as nuclease and GSH) and thermodynamic fluctuations. Moreover, the signal generation in FRET nanoflares can be easily made with ratiometric measurement, minimizing the effect of system fluctuations.

Over the past decade, gold nanoparticle (AuNP)-based fluorescently DNA probes have attracted more attentions for intracellular-specific RNA detection, because AuNPs possess many interesting properties, including distance-dependent optical features,<sup>1,2</sup> enhanced nucleic acid binding,<sup>3</sup> resistance to degradation,<sup>4</sup> and the ability to enter cells without use of transfection agents.<sup>5</sup> As far as we know, there are two main types of such AuNP-based fluorescently DNA probes: nano-beacons<sup>6–8</sup> and nanoflares.<sup>9–12</sup> Both of the probes are composed of AuNPs and single-dye-labeled DNA sequences (hairpin or linear probes), where the fluorophores are designed in close proximity to the AuNPs in the absence of targets. In the presence of targets, the targets can specifically bind and separate the fluorophores and AuNPs, resulting in recovering the fluorescence and revealing the presence of the targets (Figure S1). Several attempts have been reported using these probes to detect RNA in living cells with various degrees of success.<sup>6–12</sup> However, the single-intensity-based sensing is compromised by the local distribution of probes and by drifts of light sources and detectors. Moreover, it might generate false positive signals in a case with thermodynamic fluctuations,

glutathione (GSH) competition, nuclease degradation, or protein binding released those single-dye-labeled flares from AuNPs.<sup>13</sup>

To meet the demand for sensitive and selective detection of mRNA *in vivo* and to overcome limitations of existing AuNP-based probes, we develop a new and upgraded nanoflare, which utilizes two-fluorophore-labeled “flares” for ratiometric fluorescence measurement of mRNA in living cells based on fluorescence resonance energy transfer (FRET), since FRET involves the nonradiative transfer of energy from an excited-state fluorophore (donor) to a second chromophore (acceptor) in a close proximity (<10 nm).<sup>14</sup> FRET imaging that allows the simultaneous recording of two emission intensities at different wavelengths in the presence or absence of analytes can provide a feasible approach for precise detection.<sup>15</sup>

As illustrated in Figure 1, the newly designed probe, termed FRET nanoflares, consists of a AuNP, recognition sequences,

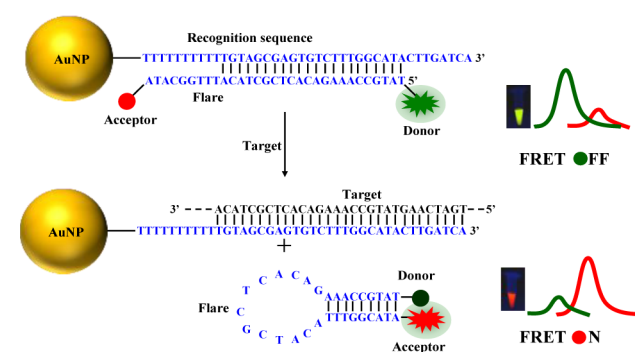


**Figure 1.** Design and working principle of the specific sequence-responsive FRET nanoflares.

and flares. Briefly, the AuNP functionalized with recognition sequences hybridized to flares are designed as hairpin structures and fluorescently labeled at their 5' and 3' termini with donors (FAM) and acceptors (TAMRA), respectively. In the absence of targets, the flares are captured by binding with the recognition sequences, separating of the donor and acceptor, and inducing low FRET efficiency. In this open state, only the fluorescence of donors can be detected. However, in the presence of targets, the flares are gradually displaced from the

Received: April 17, 2015

Published: June 25, 2015

recognition sequences by the targets, subsequently forming hairpin structures that bring the donor and acceptor into close proximity and result in high FRET efficiency. In this closed state, the fluorescence of the acceptor can be detected. Thus, the fluorescence emission ratio of acceptor to donor (A/D) can be used as a signal for quantitation of target sequences.

To prepare the FRET nanoflares, 13 nm AuNPs were prepared and functionalized with thiol-terminated recognition sequences to a specific target sequence via gold–thiol bond formation (Figure S2). These nanoconjugates were then purified and allowed to hybridize with flares. Quantification of DNA surface loading by fluorescence reveals that each AuNP contains  $\sim 85$  flares (Figure S3). To test the *in vitro* target sensing behavior of the FRET nanoflares design, we examined the response of the probes to synthetic DNA targets, instead of mRNA, at 37 °C. The results in Figure 2a showed excellent

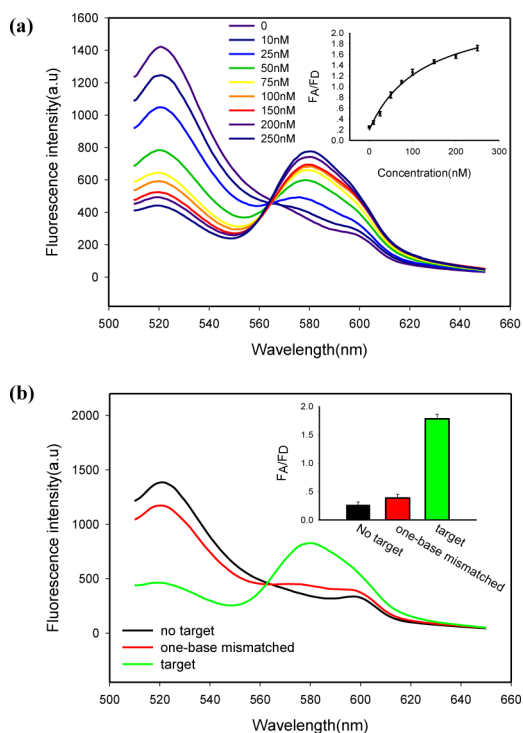


**Figure 2.** (a) Fluorescence profile of FRET nanoflares responded to different synthetic DNA targets *in vitro* at 37 °C. Inset is a plot of A/D ratio as a function of target concentrations. (b) Selectivity studies of FRET nanoflares. Inset is a histogram of A/D ratio to different targets.

FRET signal change according to different concentrations of the target. It suggested that the A/D ratio was dependent upon the target concentrations. Moreover, the results in Figure 2b demonstrated that the probes respond with a 7.0-fold increase in A/D signal upon target binding and show little increase upon one-base mismatched target DNA. These results suggested that the FRET nanoflares were efficient at signaling the presence of a specific target and also could be used to distinguish the target with a single base mismatch.

It is critical for probes to respond to their target rapidly if detecting intracellular mRNA. To investigate the rate of the flares release, we added an excess of target to a solution containing the FRET nanoflares and monitored the change in fluorescence over time (Figure S4). The results showed fluorescence of FAM decreases and TAMRA increases rapidly,

reaching completion in  $\sim 5$  min, which compares favorably to traditional nucleic acid probes such as molecular beacons.<sup>16</sup>

Compared to the conventional single-dye nanoflares,<sup>9–12</sup> the upgraded FRET nanoflares were expected to possess an excellent capability of avoiding false positive signals. The interaction of FRET nanoflares and single-dye nanoflares with Dnase I and glutathione (GSH) was then investigated, respectively. Figure 3 compared the response of FRET and

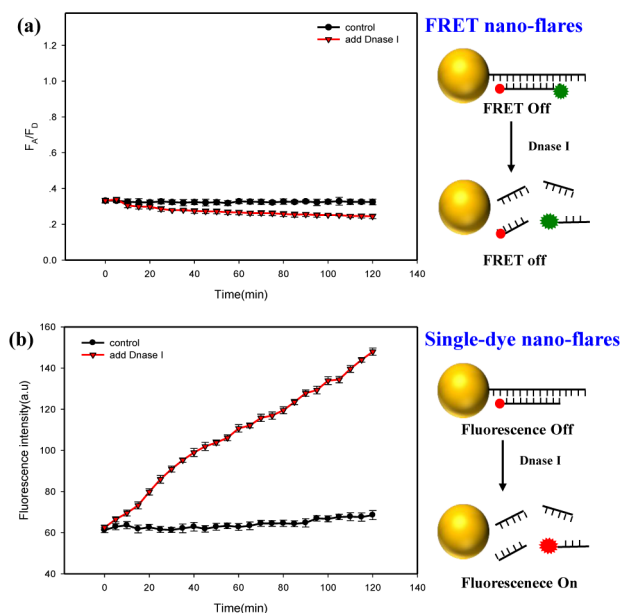


**Figure 3.** Dnase I effects on the background fluorescence signals of (a) FRET nanoflares and (b) single-dye nanoflares.

single-dye nanoflares to nuclease Dnase I, which can cleave ssDNA and dsDNA. No false positive was observed when Dnase I was added to the FRET nanoflares solution. In contrast, a gradually increasing false positive signal was detected that would be undistinguishable from a true target binding response. Similar results were observed when GSH was added to the probes solutions. Figure 4 showed that no false positive was observed when GSH was added to the FRET nanoflares solution. In contrast, a gradually increasing false positive signal after about 2 h was observed. Actually, both types of probes interacted with Dnase I and GSH, because DNAs were hydrolyzed by Dnase I and gold–thiol bonds were destroyed by GSH; even AuNPs possessed degrees of anti-enzymatic stability. The differences were that the single-dye nanoflares gave a signal change as the single-dye-labeled flares were separated from AuNPs, but the FRET nanoflares did not because the FRET pairs were not brought together; even the flares were released from AuNPs. This is critically important when the probes would be used in an intracellular environment. Furthermore, the background signals of the probes were studied with the temperature change. The results (Figure S5) showed that the fluorescence signals of the FRET nanoflares displayed a stable and low background and the single-dye nanoflares revealed a gradual increase with rising temperatures, in the absence of targets. The unusual behavior suggested that the FRET signal was much less dependent on temperature than the single-dye nanoflares.

To investigate the intracellular mRNA detection, we chose TK1 mRNA as a target, which is associated with cell division

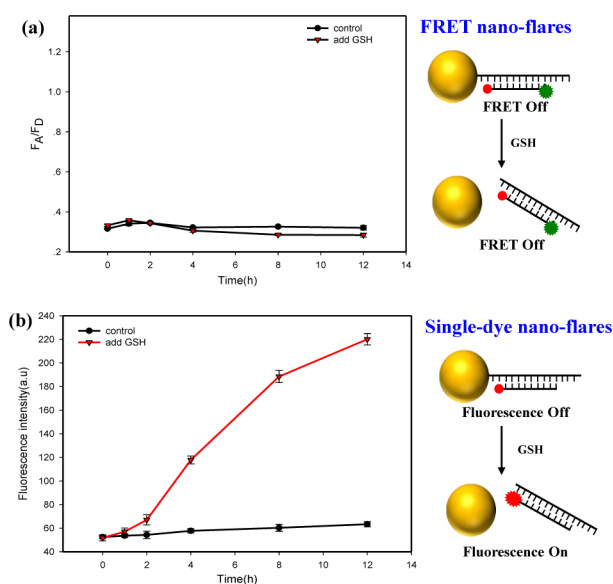


**Figure 4.** GSH effects on the background fluorescence signals of (a) FRET nano-flares and (b) single-dye nano-flares.

and is proposed to be a marker for tumor growth.<sup>17,18</sup> In this work, HepG2 (human liver hepatocellular carcinoma cell line) and MCF-7 (breast cancer cell line) were selected as the positive cells, and L02 (normal human hepatocyte cell line) was selected as the negative cell. The relative high expression levels of TK1 mRNA in these three cell lines were determined in the reported literature and showed that the L02 cell line has a lower TK1 mRNA expression level than the HepG2 and MCF-7 cell lines.<sup>8,12</sup> First, cellular uptake study of the FRET nano-flares was performed. Following incubation with L02 and HepG2 cell lines, most particles resided in cytosol as individual particles or clusters, as evidenced by TEM imaging data (Figure S6). Moreover, the fluorescence colocalization imaging data of HepG2 cell lines (Figure S7) also showed that the FRET nano-flares were distributed in the cytoplasm, ensuring the chance to approach the cytoplasmic mRNA. Second, the incubation time of the FRET nano-flares was studied with HepG2 and L02 cell lines. ICP-MS data (Figure S8) showed that the amounts of intracellular AuNPs were gradually increased with the incubation time until saturation at about 2.5–3.0 h, which also suggested that there were relatively equal numbers of particles in HepG2 and L02 cell lines. Furthermore, the fluorescence imaging data (Figure S9) showed that the FRET signals (red color) in HepG2 cells were gradually increased with the incubation time until 2.5 h and then gradually faded, but the FRET signals in L02 cells were very low, at all times, under the same conditions. It suggested that the 2.5 h incubation time should be appropriate for use in the following experiments and that the released flares might be degraded by the intracellular environment after 2.5 h incubation.

It is important to investigate the specificity of the FRET nano-flares in living cells. A control probe (nonrecognition sequence) containing a mismatched recognition sequence (three base substitutions) was prepared. HepG2 cells were incubated with recognition FRET nano-flares and control probes and then imaged using scanning confocal microscopy. The results (Figure S10) showed that HepG2 cells treated with recognition FRET nano-flares were highly red fluorescent as compared to those treated with control probes. Further,

different types of cell lines were selected to study the specificity of the FRET nano-flares. Figure 5 showed the fluorescence

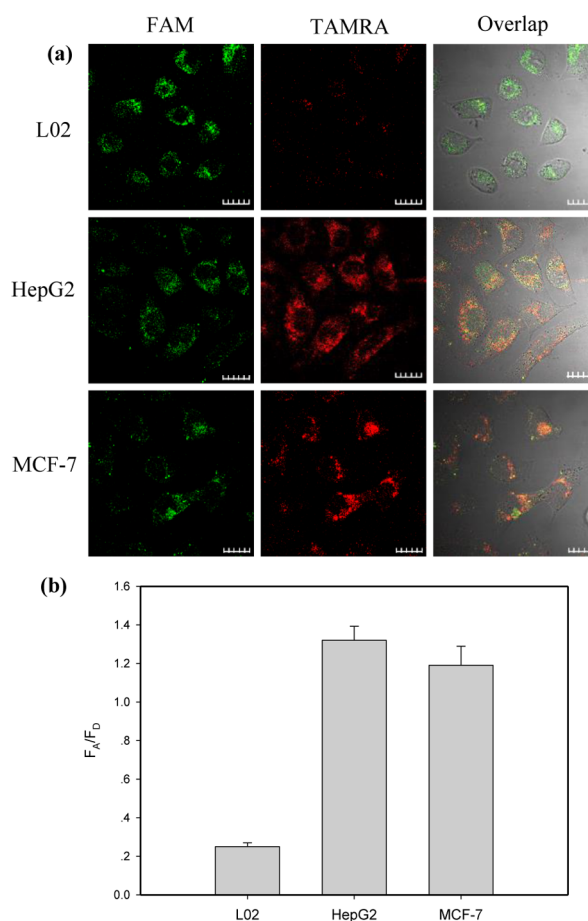


**Figure 5.** (a) Fluorescence images of TK1 mRNA in L02, HepG2, and MCF-7 cells by FRET nano-flares. Scale bars are 20  $\mu\text{m}$ . (b) Histogram of the relative fluorescence intensity (A/D) of the above three cell lines.

images of TK1 mRNA by incubating FRET nano-flares with two positive cell lines (HepG2, MCF-7) and one negative cell line (L02) for 2.5 h, respectively. It showed that strong FRET signals (red fluorescence) for TK1 mRNA in HepG2 and MCF-7 were observed, and almost no red fluorescence in L02 was detected. The results were consistent with the results of another conventional technique qRT-PCR (Figure S11) and further indicated that the signals of the FRET nano-flares were correlated very well with the levels of mRNA expression.

The expression levels of mRNA in cancer cells are different in the various stages of tumor progression. It is critical to determine the relative expression levels of mRNA for cancer detection and therapy. TK1 mRNA in HepG2 was chosen as an example. It was reported that tamoxifen induced the down regulation of TK1 mRNA expression.<sup>19,20</sup> HepG2 cells were divided into two groups: One group was treated with tamoxifen to decrease the TK1 mRNA expression, and the other was untreated, which served as a control. Figure 6 showed that the red fluorescence was lower in the tamoxifen treated HepG2 cells relative to that in the untreated cells. qRT-PCR further confirmed that the level of TK1 mRNA expression decreased after tamoxifen treatment (Figure S12). These results indicated that the fluorescence intensity correlated well with the level of

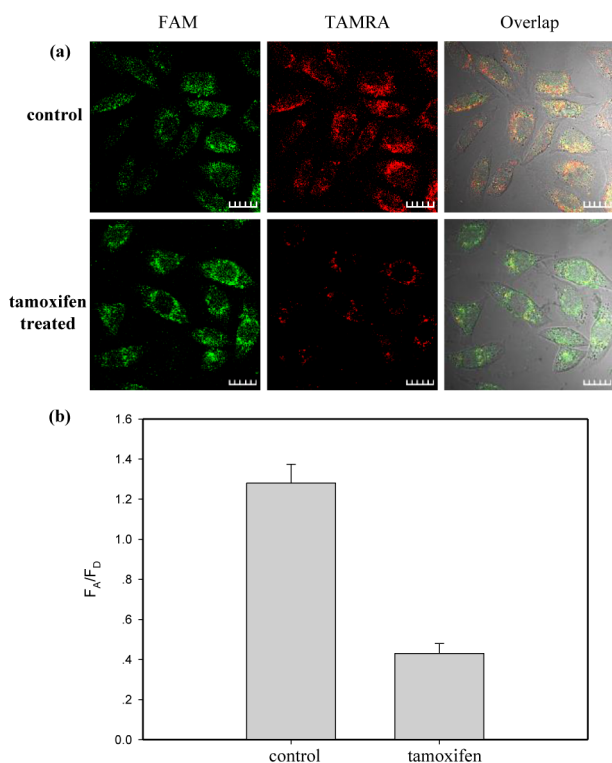


**Figure 6.** (a) Fluorescence images of TK1 mRNA in HepG2 cells treated without and with tamoxifen by FRET nanoflares. Scale bars are 20  $\mu\text{m}$ . (b) Histogram of the relative fluorescence intensity (A/D) of the above two groups.

tumor-related mRNA expression in living cells. Thus, the FRET nanoflares are capable of detecting changes in gene expression levels in cancer cells.

In summary, we have presented a new class of intracellular nanoprobe termed FRET nanoflares. They possess the merits of conventional single-dye nanoflares, such as cellular transfection, stability, and fluorescence superquenching. Moreover, compared to the conventional nanoflares, the upgraded FRET nanoflares have their own advantages. First, they do not generate any false positive signals upon thermodynamic fluctuations and chemical interferences (such as nuclease and GSH). Second, the signal generation in FRET nanoflares can be easily made with ratiometric measurement, minimizing the effect of system fluctuations. Of course, the FRET nanoflares also have potential drawbacks including the need for dual-fluorophore labeled and more complicated probe design because each must contain a self-complementary region as well as a target region. We think, with different recognition elements (such as aptamers) in engineering FRET nanoflares, the ratiometric sensing strategy could potentially be applied to create a variety of new multicolor sensors for intracellular detection. The experiments on FRET nanoflares for other targets are being conducted in our laboratory, and the results will be reported in due course.

## ■ ASSOCIATED CONTENT

### 📄 Supporting Information

Procedures and additional data. The Supporting Information is available free of charge on the ACS Publications website at DOI: 10.1021/jacs.5b04007.

## ■ AUTHOR INFORMATION

### Corresponding Author

\*kmwang@hnu.edu.cn.

### Author Contributions

‡These authors contributed equally to this work.

### Notes

The authors declare no competing financial interest.

## ■ ACKNOWLEDGMENTS

This work was supported by the National Natural Science Foundation of China (21190044, 21205032), Hunan Provincial Natural Science Foundation of China (13JJ4032), International Science & Technology Cooperation Program of China (2010DFB30300), and the Fundamental Research Funds for the Central Universities.

## ■ REFERENCES

- (1) Dulkeith, E.; Ringler, M.; Klar, T. A.; Feldmann, J.; Javier, A. M.; Parak, W. J. *Nano Lett.* **2005**, *5*, 585.
- (2) Storhoff, J. J.; Lazarides, A. A.; Mucic, R. C.; Mirkin, C. A.; Letsinger, R. L.; Schatz, G. C. *J. Am. Chem. Soc.* **2000**, *122*, 4640.
- (3) Lytton-Jean, A. K. R.; Mirkin, C. A. *J. Am. Chem. Soc.* **2005**, *127*, 12754.
- (4) Seferos, D. S.; Prigodich, A. E.; Giljohann, D. A.; Patel, P. C.; Mirkin, C. A. *Nano Lett.* **2009**, *9*, 308.
- (5) Giljohann, D. A.; Seferos, D. S.; Patel, P. C.; Millstone, J. E.; Rosi, N. L.; Mirkin, C. A. *Nano Lett.* **2007**, *7*, 3818.
- (6) Song, S.; Liang, Z.; Zhang, J.; Wang, L.; Li, G.; Fan, C. *Angew. Chem., Int. Ed.* **2009**, *48*, 8670.
- (7) Jayagopal, A.; Halfpenny, K.; Perez, J.; Wright, D. *J. Am. Chem. Soc.* **2010**, *132*, 9789.
- (8) Pan, W.; Zhang, T.; Yang, H.; Diao, W.; Li, N.; Tang, B. *Anal. Chem.* **2013**, *85*, 10581.
- (9) Seferos, D. S.; Giljohann, D. A.; Hill, H. D.; Prigodich, A. E.; Mirkin, C. A. *J. Am. Chem. Soc.* **2007**, *129*, 15477.
- (10) Prigodich, A. E.; Seferos, D. S.; Massich, M. D.; Giljohann, D. A.; Lane, B. C.; Mirkin, C. A. *ACS Nano* **2009**, *3*, 2147.
- (11) Prigodich, A. E.; Randeria, P. S.; Briley, W. E.; Kim, N. J.; Daniel, W. L.; Giljohann, D. A.; Mirkin, C. A. *Anal. Chem.* **2012**, *84*, 2062.
- (12) Li, N.; Chang, C.; Pan, W.; Tang, B. *Angew. Chem., Int. Ed.* **2012**, *51*, 7426.
- (13) Rosi, N. L.; Giljohann, D. A.; Thaxton, C. S.; Lytton-Jean, A. K. R.; Han, M. S.; Mirkin, C. A. *Science* **2006**, *312*, 1027.
- (14) Roy, R.; Hohng, S.; Ha, T. A. *Nat. Methods* **2008**, *5*, 507.
- (15) Chen, H. H.; Ho, Y. P.; Jiang, X.; Mao, H. Q.; Wang, T. H.; Leong, K. W. *Nano Today* **2009**, *4*, 125.
- (16) Wang, K.; Tang, Z.; Yang, C.; Kim, Y.; Fang, X.; Li, W.; Wu, Y.; Medley, C.; Cao, Z.; Li, J.; Colon, P.; Lin, H.; Tan, W. *Angew. Chem., Int. Ed.* **2009**, *48*, 856.
- (17) Broet, P.; Romain, S.; Daver, A.; Ricolleau, G.; Quillien, V.; Rallet, A.; Asselain, B.; Martin, P. M.; Spyrtos, F. *J. Clin. Oncol.* **2001**, *19*, 2778.
- (18) Chen, C.; Chang, T.; Chen, F.; Hou, M.; Hung, S.; Chong, L.; Lee, S.; Zhou, T.; Lin, S. *Oncology* **2006**, *70*, 438.
- (19) Kasid, A.; Davidson, N. E.; Gelmann, E. P.; Lippman, M. E. *J. Biol. Chem.* **1986**, *261*, 5562.
- (20) Foekens, J. A.; Romain, S.; Look, M. P.; Martin, P. M.; Klijn, J. G. M. *Cancer Res.* **2001**, *61*, 1421.